DTU Library

Gain-switched all-fiber laser with narrow bandwidth

Larsen, Casper; Giesberts, M.; Nyga, S.; Fitzau, O.; Jungbluth, B.; Hoffmann, H. D.; Bang, Ole

[Link back to DTU Orbit](#)

Gain-switched all-fiber laser with narrow bandwidth

C. Larsen,[1,*] **M. Giesberts,**[2] **S. Nyga,**[2] **O. Fitzau,**[2] **B. Jungbluth,**[2]
H. D. Hoffmann,[2] **and O. Bang**[1,3]

[1]*DTU Fotonik, Department of Photonics Engineering, Technical University of Denmark,*
2800 Kgs. Lyngby, Denmark
[2] *Fraunhofer-Institute for Lasertechnology, Steinbachstrasse 15, 52074 Aachen, Germany,*
[3] *NKT Photonics A/S, Blokken 84, DK-3460, Birkerød, Denmark*
*crla@fotonik.dtu.dk

Abstract: Gain-switching of a CW fiber laser is a simple and cost-effective approach to generate pulses using an all-fiber system. We report on the construction of a narrow bandwidth (below 0.1 nm) gain-switched fiber laser and optimize the pulse energy and pulse duration under this constraint. The extracted pulse energy is 20 μJ in a duration of 135 ns at 7 kHz. The bandwidth increases for a higher pump pulse energy and repetition rate, and this sets the limit of the output pulse energy. A single power amplifier is added to raise the peak power to the kW-level and the pulse energy to 230 μJ while keeping the bandwidth below 0.1 nm. This allows frequency doubling in a periodically poled lithium tantalate crystal with a reasonable conversion efficiency.

References and links

1. D. J. Richardson, J. Nilsson, and W. A. Clarkson, "High power fiber lasers: current status and future perspectives [invited]," J. Opt. Soc. Am. B **27**, B63–B92 (2010).
2. A. Tünnermann, T. Schreiber, and J. Limpert, "Fiber lasers and amplifiers: an ultrafast performance evolution," Appl. Opt. **49**, F71–F78 (2010).
3. M. E. Fermann, M. J. Andrejco, Y. Silberberg, and M. L. Stock, "Passive mode locking by using nonlinear polarization evolution in a polarization-maintaining Erbium-doped fiber," Opt. Lett. **18**, 894–896 (1993).
4. T. V. Andersen, P. Pérez-Millán, S. R. Keiding, S. Agger, R. Duchowicz, and M. V. Andrés, "All-fiber actively Q-switched Yb-doped laser," Opt. Commun. **260**, 251–256 (2006).
5. M. V. Andrés, J. L. Cruz, A. Diez, P. Pérez-Millán, and M. Delgado-Pinar, "Actively Q-switched all-fiber lasers," Laser Phys. Lett. **5**, 93–99 (2008).
6. A. S. Kurkov, "Q-switched all-fiber lasers with saturable absorbers," Laser Phys. Lett. **8**, 335–342 (2011).
7. D. B. S. Soh, S. E. Bisson, B. D. Patterson, and S. W. Moore, "High-power all-fiber passively Q-switched laser using a doped fiber as a saturable absorber: numerical simulations," Opt. Lett. **36**, 2536–2538 (2011).
8. S. V. Chernikov, Y. Zhu, J. R. Taylor, and V. P. Gapontsev, "Supercontinuum self-Q-switched ytterbium fiber laser," Opt. Lett. **22**, 298–300 (1997).
9. J. Ding, B. Sampson, A. Carter, C. Wang, and K. Tankala, "A monolithic Thulium doped single mode fiber laser with 1.5 ns pulsewidth and 8kW peak power," in "Proc. SPIE," (2011), 79140X.
10. M. Jiang and P. Tayebati, "Stable 10 ns, kilowatt peak-power pulse generation from a gain-switched Tm-doped fiber laser," Opt. Lett. **32**, 1797–1799 (2007).
11. C. Larsen, D. Noordegraaf, P. M. W. Skovgaard, K. P. Hansen, K. E. Mattsson, and O. Bang, "Gain-switched CW fiber laser for improved supercontinuum generation in a PCF," Opt. Express **19**, 14883–14891 (2011).
12. C. Larsen, S. T. Sørensen, D. Noordegraaf, K. P. Hansen, K. E. Mattsson, and O. Bang, "Zero-dispersion wave-length independent quasi-CW pumped supercontinuum generation," Opt. Commun. **290**, 170 – 174 (2013).
13. S. D. Jackson and T. A. King, "Efficient gain-switched operation of a Tm-doped silica fiber laser," IEEE J. Quantum Electron. **34**, 779–789 (1998).

14. L. A. Zenteno, E. Snitzer, H. Po, R. Tumminelli, and F. Hakimi, "Gain switching of a Nd^{3+}-doped fiber laser," Opt. Lett. **14**, 671 (1989).
15. K.S. Wu, D. Ottaway, J. Munch, D. G. Lancaster, S. Bennetts, and S. D. Jackson, "Gain-switched Holmium-doped fibre laser," Opt. Express **17**, 20872–20877 (2009).
16. Y. Sintov, M. Katz, P. Blau, Y. Glick, E. Lebiush, Y. Nafcha, and N. Soreq, "A frequency doubled gain switched Yb3+ doped fiber laser," in "Proc. SPIE," (2009), 7195.
17. M. Giesberts, J. Geiger, M. Traub, and H. D. Hoffmann, "Novel design of a gain-switched diode-pumped fiber laser," in "Proc. of SPIE," (2009), 71952.
18. R. Petkovšek, V. Agrež, F. Bammer, P. Jakopič, and B. Lenardič, "Experimental and theoretical study of gain switched Yb-doped fiber laser," in "Proc. SPIE," (2013), 8601.
19. D. G. Carlson, "Dynamics of a repetitively pump-pulsed Nd: YAG laser," J. Appl. Phys. **39**, 4369–4374 (1968).
20. P. Wan, J. Liu, L. Yang, and F. Amzajerdian, "Low repetition rate high energy 1.5 μm fiber laser," Opt. Express **19**, 18067–18071 (2011).
21. A. Starodoumov and N. Hodgson, "Harmonic generation with fiber MOPAs and solid state lasers – technical challenges, state-of-the-art comparison and future developments," in "Proc. SPIE," (2011), 79120H.
22. B. Jungbluth, S. Nyga, E. Pawlowski, T. Fink, and T. Wueppen, "Efficient frequency conversion of pulsed microchip and fiber laser radiation in PPSLT," in "Proc. SPIE," (2011), 79120K.
23. S. Nyga, J. Geiger, and B. Jungbluth, "Frequency doubling of fiber laser radiation of large spectral bandwidths," in "Proc. SPIE," (2010), 75780P.

1. Introduction

Rare-earth doped fiber lasers and amplifiers have emerged as technologies with a wide spectrum of applications ranging from material processing to telecommunication. Owing to mass-produced high-power pump diodes, the double-clad pumping geometry, and a low quantum defect, multiple kilowatts of output power with diffraction-limited beam quality is commercially available [1, 2]. Another important advantage of fiber lasers is that it is possible to completely avoid free-space components, which require careful alignment and are sensitive to vibrations. Fiber lasers that are constructed only of fiber-based components all the way from the fiber-coupled pump diodes to the laser output are known to be maintenance-free, highly reliable, compact, and robust. It is however rather challenging to make stable pulsed lasers in an all-fiber manner.

Examples of methods of pulsing an all-fiber laser are mode-locking, Q-switching, and gain-switching. Femtosecond pulses can be produced by mode-locking through the use of nonlinear polarization rotation [3]. Active Q-switching has been achieved by detuning the cavity through elongation of one of the fiber Bragg gratings [4,5]. Passive Q-switching has been demonstrated with specially-doped or standard small-mode-area saturable absorber fibers [6, 7]. The fiber geometry allows for a very high single pass gain of more than 50 dB, which is advantageous in amplifiers. However, the high gain increases the requirements for the contrast of a Q-switching element and is the origin of often destructive self-pulsation [8].

Gain-switching makes use of the inherent relaxation oscillations of the fiber laser by fast modulation of the pump. In terms of optical components a gain-switched fiber laser only requires the same components as an all-fiber CW laser, which makes it simple and cost-effective. Output pulse energies are typically in the tens to hundreds of microjoule range and with nanosecond pulse duration [9–11]. An example of an application is within supercontinuum generation [11], where the increased peak power reduces the dependence on the zero dispersion wavelength [12]. One downside of gain-switching is that the full capacity of the pump lasers is not utilized due to the pulsed pumping. Gain-switching is studied the most in Tm-doped lasers [9,10,13] but it has also been demonstrated in Nd-doped [14], Ho-doped [15], and Yb-doped fiber lasers [11, 16–18].

Here we report on the construction of a simple, gain-switched, Yb-doped fiber laser with a narrow bandwidth. We present, to our knowledge, the first thorough characterization of the bandwidth versus pulse energy and repetition rate of such a gain-switched fiber laser. The op-

timum point of operation for extracting the highest pulse energy while keeping the bandwidth below 0.1 nm is found. For many nonlinear conversion applications a peak power in the kilowatt range is needed, and therefore we set a goal of reaching more than a kilowatt of peak power. Finally we demonstrate an application of the laser, namely frequency doubling in a nonlinear crystal.

2. The experimental setup

The experimental setup is illustrated in Fig. 1. An electronic trigger activates the diode driver (Picolas GmbH) and the 915 nm pump diodes deliver short pump pulses (100-700 ns) at low repetition rates (1-10 kHz). Cladding pumped fibers with a numerical aperture of 0.46 and an outer diameter of 125 μm are used. To obtain linearly polarized output all components are polarization maintaining, and the active fiber is coiled.

(a) All-fiber Master Oscillator (MO)
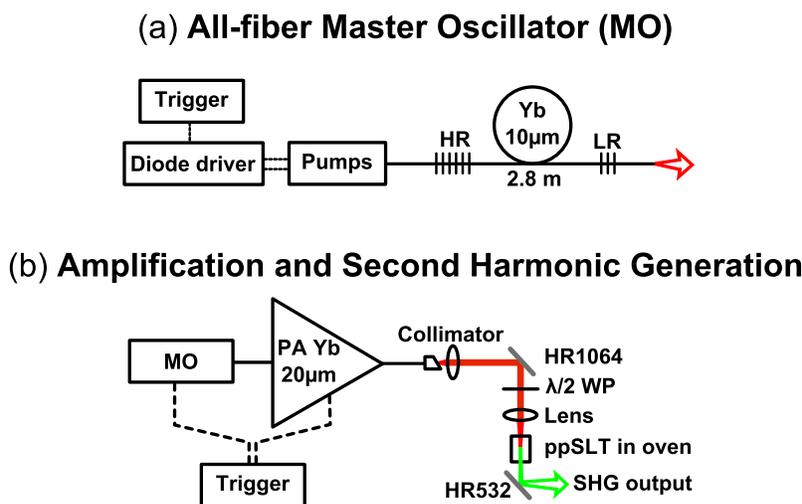
(b) Amplification and Second Harmonic Generation

Fig. 1. The setup of the fiber laser and the SHG experiment. See text for explanations.

The master oscillator (MO) consists of a single-mode 10 μm core Yb-doped double clad fiber with a length of 2.8 m, pump absorption of 1.7 dB/m at 915 nm, and a high birefringence of 3×10^{-4}, which facilitates linearly polarized operation when coiled. The active fiber is spliced in-between the high reflectance (HR) and the low reflectance (LR) fiber Bragg gratings. The bandwidth of the HR is 0.6 nm with a reflectivity of >99% and the LR has a 3 dB bandwidth of 0.185 nm and a peak reflectivity of 13.7%.

The diode pumps of the power amplifier (PA) are synchronously triggered with the MO. The used pump diodes can deliver up to four times higher power than the nominal when they are turned on for less than $\sim$1 μs. The PA is made of 1.75 m of 20 μm core fiber with a pump absorption at 915 nm of 7 dB/m and a birefringence of 1.1×10^{-4}, and it is forward and backward pumped. The output fiber facet is angle cleaved and the beam is collimated. There is no need for isolators due to the large fiber core in the MO, and all the pump diodes are protected by only weak coupling of the core light to the combiner ports.

Second harmonic generation (SHG) is carried out in a commercially available, bulk, periodically poled stoichiometric lithium tantalate (ppSLT) crystal with a length of 10 mm, an aperture of 1x3 mm, and a poling period of 8 μm. The temperature is controlled in an oven with an accuracy of 0.01°C to maintain phasematching. The fiber output is reflected off a dichroic mirror with high reflection for the signal wavelength (HR1064), and is transmitted through a half-wave

plate ($\lambda/2$ WP) before being focused onto the ppSLT crystal. Thereby any residual pump light at 915 nm is removed and the polarization can be aligned to the crystal axis. The focal length is 75 mm and the diameter at the focus is 110 μm (e^{-2}), which means that the intensity is well below the damage threshold of the coating on the crystal. The frequency doubled output is filtered by dichroic mirrors with high transmission at 1064 nm and high reflection at 532 nm (HR532).

3. Gain-switching of the fiber laser

In gain-switching the pump of a laser is modulated to provoke spiking of the laser [19]. The dynamics is outline in Fig. 2(a). When the pumping of the laser medium is initiated, the density of excited ions quickly creates population inversion in the quasi-four level system. Amplification of the spontaneous emission occurs until the optical power in the cavity starts to deplete the population inversion. The pump is turned off before the generated spike is emitted to avoid the following smaller spikes. The generated pulse duration, energy, and build-up time depend on pump energy, cavity design, and repetition rate [11, 17].

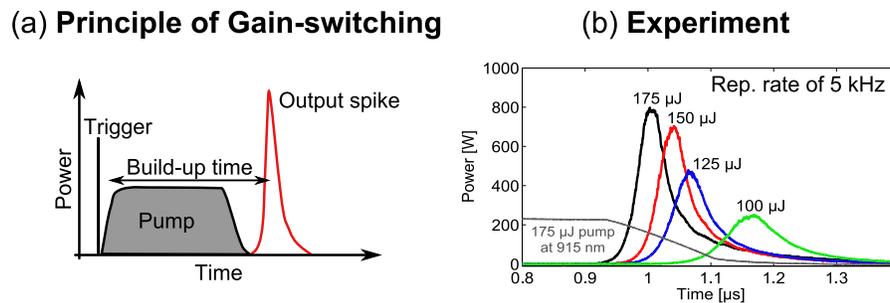(a) **Principle of Gain-switching**   (b) **Experiment**

Fig. 2. Gain-switching of the fiber laser. (a) Schematics of gain-switching. (b) Output pulses for increased absorbed pump energy at a fixed repetition rate of 5 kHz. The tail of the 915 nm pump pulse with energy of 175 μJ is shown in gray.

The output pulses of the gain-switched fiber laser are shown in Fig. 2(b) for increasing absorbed pump energy and at a fixed repetition rate of 5 kHz. It can be seen that increasing the absorbed pump energy increases the output peak power and decreases the build-up time and pulse duration. The build-up time turns out to scale approximately as the reciprocal of the square root of the pump pulse energy [19]. In order to continue raising the pump energy without any temporal overlap of the pump and output pulse, an increased pump capacity (power) is required. In fact, at the absorbed pump energy of 175 μJ the emission of the spike occurs before the pump pulse has ended, which can be seen in Fig. 2(b). This situation degrades the temporal pulse shape by transfer of energy from the peak to the tail of the pulse. Therefore, in order to avoid this, the energy of the pump pulse should be no higher than 150 μJ at 5 kHz.

In Fig. 3(a) the temporal traces of the pump and the emitted spikes are shown for a fixed absorbed pump energy of 150 μJ and at repetition rates from 1 kHz to 5 kHz. The lowest repetition rates imply that the delay between the pump pulses are on the order of the lifetime of the excited Yb-ions ($f^{-1} \sim \tau_{Yb}$) of around 1 ms [11]. The amount of residual excited Yb-ions still present when a new pump pulse arrives is therefore dependent on the repetition rate. This causes a higher population inversion at the time of spike emission for higher repetition rates, which leads to higher pulse energy, higher peak power, and shorter pulse duration. At the repetition rate of 5 kHz the output pulses have a duration of 66 ns, a peak power of 700 W, a pulse energy of 55.4 μJ, and as the absorbed pump energy is 150 μJ the optical-to-optical efficiency is 36%.
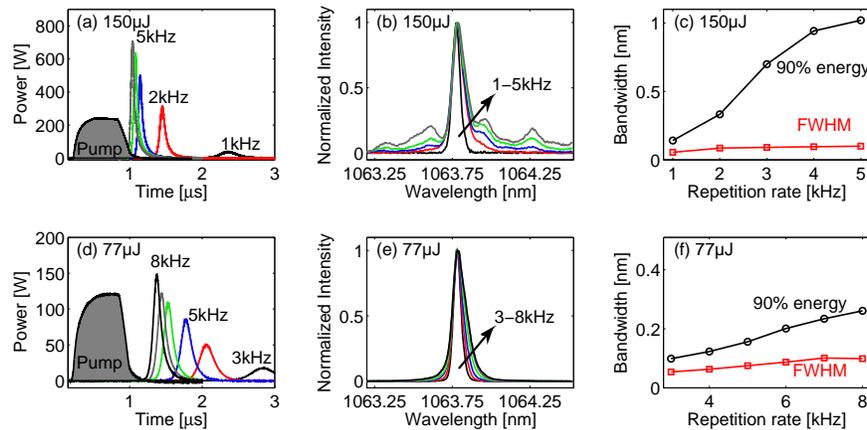
Fig. 3. Characterization of the output of the MO at increasing repetition rate and absorbed pump energies. Temporal pulse shapes are shown in (a) and (d) for 150 μJ and 77 μJ absorbed pump energies, respectively. The spectra are given in (b) and (e). Calculated FWHM and 90%-confined-energy bandwidths are shown at increasing repetition rate in (c) and (f).

The normalized spectra of the output pulses are shown in Fig. 3(b) for increasing repetition rate. At the lowest repetition rate of 1 kHz the spectrum has a narrow Gaussian-like shape. The spectra at higher repetition rates have, besides a narrow central peak, irregular and broad structures that contain a significant amount of the pulse energy. The commonly used full-width half-maximum (FWHM) is not a good measure of the actual bandwidth of these pulses. We have found that in addition to using the FWHM, the bandwidth that contains 90% of the pulse energy (B90) must be evaluated. For a Gaussian spectral shape the B90 is 1.4 times the FWHM and for a Lorentzian shape the B90 is a factor of five of the FWHM. The ratio of the B90 and the FWHM can be seen as a measure of the quality of the spectrum. In Fig. 3(c) the FWHM and B90 bandwidths are shown for increasing repetition rate. At the lowest repetition rate of 1 kHz the spectrum has a narrow FWHM of 0.055 nm and a B90 of 0.14 nm. At the highest repetition rate of 5 kHz the FWHM increases slightly to 0.1 nm while the B90 reaches 1 nm. The reason for this is that the gain becomes so high that lasing occurs at wavelengths, which are hardly supported by the cavity.

The constraint of a narrow and high quality spectrum therefore sets a limit on the tolerable gain. To have a small B90 either the repetition rate or the pump energy can be reduced. In Fig. 3(c) the B90 is low for a repetition rate of 1 kHz, however the efficiency is reduced to less than 10% due to the large decay of the excited ions between pump pulses. To obtain a better efficiency the repetition rate must be several kilohertz and hence the pump energy must be reduced.

In Fig. 3(d) The temporal pulse shapes are shown for a reduced absorbed pump energy of 77 μJ. The repetition rate is varied between 3 kHz and 8 kHz, resulting in an output pulse with a duration of 130 ns, a peak power of 150 W, a pulse energy of 22.4 μJ, and as the absorbed pump energy is 77 μJ the optical-to-optical efficiency is 30% at 8 kHz. At a repetition rate of 4 kHz the efficiency is half of this value due to the relaxation of excited Yb-ions. In contrast to pumping with a pulse energy of 150 μJ, the spectra at 77 μJ stay well-behaved at increased repetition rate, which also results in a smaller B90 of maximum 0.25 nm at 8 kHz. The polarization extinction ratio (PER) is 14 dB.

As the peak power increases while the B90 degrades with the repetition rate, the optimum

repetition rate is a trade-off between spectral quality and power. We have chosen the repetition rate of 7 kHz, there the peak power is 120 W, the FHWM is 0.1 nm, and B90 is 0.23 nm. The pulse duration is 135 ns and the pulse energy is 20 μJ, which corresponds to an efficiency of 26%.

Realizations of Yb-doped gain-switched fiber lasers in the literature have reached pulses with energy of 16 μJ and 125 ns duration contained in a FWHM bandwidth of 0.2 nm (B90 is approximately 0.4 nm) [16] and longer pulses of 200 ns duration with energy of 150 μJ and FWHM bandwidth of 0.4 nm [11]. We have therefore demonstrated a low record FWHM bandwidth of 0.1 nm and a record pulse duration of 66 ns with 150 μJ of absorbed pump energy, however the spectral quality is poor with a B90 of 1 nm. For the absorbed energy of 77 μJ a much better spectral quality is achieved and still with a low FWHM bandwidth of 0.1 nm and a pulse duration of 135 ns, which is only slightly longer than in [16]. Our smaller bandwidth can be attributed to that the study in [16] used a LR grating with twice the bandwidth and about three times smaller reflectance.

During the experiments we did not observe any instabilities of the output pulse such as pulse stacking [15]. We use in-band pumping which is characterized by a rapid decay from the pumping level to the upper lasing-level and it enables high energy extraction that stabilize the operation.

Another important result from our design optimization of a narrow bandwidth gain-switched laser is that the effect of bandwidth broadening restricts the maximum obtainable peak power to well below the kilowatt level, which motivates the use of amplification to reach the target of narrow bandwidth and a peak power in the kilowatt range.

4. Pulse-pumped power amplification

To reach our target peak power the output pulse must be amplified by more than 10 dB without significant degradation of the polarization or bandwidth. To overcome the limitation of amplified spontaneous emission (ASE) and catastrophic self-pulsation of the amplifier at the low repetition rate we chose to use a pulse-pumped power amplification scheme [8, 20].

The results of the amplification are shown in Fig. 4 and in Table 1. For the seed pulse energy of 20 μJ and the repetition rate of 7 kHz the power amplifier (PA) shows transparency at 89 μJ of absorbed PA pump energy, a high slope efficiency of 63%, and an optical-to-optical efficiency up to 50%. The pulse duration increases to around 150 ns, the peak power is more than 1.4 kW, and the output pulse energy is 230 μJ for the absorbed PA pump energy of 425 μJ. The FWHM bandwidth is unchanged at 0.1 nm but the B90 increases to 0.33 nm. The residual pump light at 915 nm and unpolarized signal light are as low as 15% of the output power. The PER is better than 11 dB and no ASE is observed. The 20 μm core of the amplifier ensures that the peak intensity is well below the threshold of nonlinear effects in the amplifier, such as stimulated Raman scattering.

Table 1. The pump, amplified 1064 nm output, and 532 nm pulse energies are shown together with the SHG efficiency.

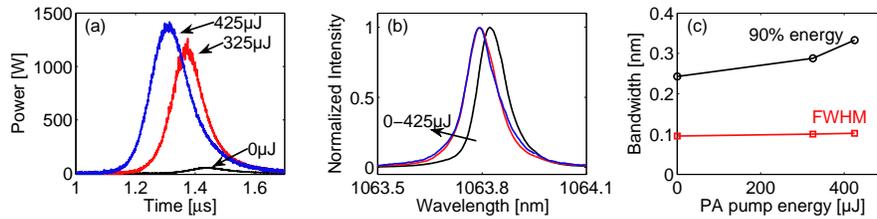| Power amplification		Second harmonic generation	
Pump energy, μJ	1064 nm energy, μJ	532 nm energy, μJ	SHG efficiency, %
220	100	31	31
325	164	57	35
425	230	84	37

Fig. 4. Pulse-pumped amplification of the MO output at 7 kHz. The temporal shapes, the spectra, and FWHM and 90%-confined-energy bandwidths are shown with increasing absorbed PA pump energy in (a), (b), and (c), respectively.

5. Application: Second Harmonic Generation

The output pulse of our amplified, gain-switched fiber laser is suitable for frequency conversion such as second harmonic generation (SHG). To demonstrate this application we have conducted a simple SHG experiment. Challenges and limits of efficient frequency conversion of fiber lasers are discussed in [21–23]. The filtered output from the PA is focus into the ppSLT crystal. In Table 1 the 532 nm output pulse energies are shown for the different input pulse energies. The conversion efficiency increases with the pulse energy and at the highest pulse energy tested of 230 μJ, corresponding to a peak power of 1.4 kW, the 532 nm pulse energy is 84 μJ and the efficiency reaches 37%.

The setup was designed to show the feasibility of the gain-switched fiber laser as a seed and hence not designed to handle a high thermal load, which turned out to limit power scaling. Therefore, the reported SHG result are not obtained at the full pump capacity and with low peak intensity <25 MW/cm^2 in the nonlinear crystal. This is far below the threshold of bulk and surface damage of the ppSLT crystal. We believe that a higher conversion efficiency can be obtained by increasing the amplification factor and by a tighter focusing of the beam.

6. Conclusion

We have demonstrated gain-switching of a fiber laser to produce narrow bandwidth, short duration, and high energy pulses. This approach has the advantage of being all-fiber and only consist of highly reliable standard fiber components. By driving the gain-switched laser at 7 kHz we achieved a pulse energy of 20 μJ in a duration of 135 ns with a FWHM bandwidth of 0.1 nm and high spectral quality. By increasing the repetition rate or the pump energy the bandwidth increased due to a too high gain, which caused lasing at wavelengths hardly supported by the cavity. This effect of bandwidth broadening restricts the maximum obtainable peak power to well below the kilowatt level, which motivates the use of power amplification to reach a peak power of more than a kilowatt. After amplification a peak power of 1.4 kW and an unchanged FWHM bandwidth of 0.1 nm were achieved. These pulses were sufficient for efficient second harmonic generation in a periodically poled quasi-phasematched stoichiometric lithium tantalate crystal and a conversion efficiency of 37% was reached resulting in 84 μJ 532 nm pulses at 7 kHz.